Numerical Prediction of Airflow and Temperature Distribution in Large-Scale Agricultural PVC Greenhouse

Keita Hattori[1] and Kazuhide Ito[2]

[1] Graduate student, IGSES, Kyushu University, Fukuoka, Japan
[2] IGSES, Kyushu University, Fukuoka, Japan

Abstract

Large-scale greenhouses are usually adopted to control the indoor climate conditions in agriculture. The envelope of agricultural greenhouses generally consists of a PVC (polyvinyl chloride) sheet, which produces a so-called greenhouse effect and protection from harmful insects. In winter, a supplementary heating device in greenhouses is needed because of the lower outdoor temperature and the non-uniform distribution of indoor temperature. Existing research concerning indoor environmental conditions formed in PVC greenhouses is insufficient and precise numerical predictions of airflow and temperature distribution in large-scale vinyl houses are important to develop effective designs from the viewpoint of energy-saving and the development of suitable indoor environments for agricultural products.

To this end, coupled numerical analysis of CFD (computational fluid dynamics) and air-conditioning system was also carried out and the sensor position in the greenhouse and operation of a stirred fan were confirmed to have great impact on energy consumption.

Keywords: PVC greenhouse, CFD, Stirred fan, Flow and temperature distribution

Introduction

Greenhouses are widely used throughout the world owing to the ease of control of indoor environment, low cost, and simple structure. However, during the night-time in winter,

supplementary heating equipment, namely, a hot-air furnace system or other air-heating devices, may be necessary to control the cultivation temperature in PVC greenhouses when the outside temperature decreases rapidly. For large-scale PVC greenhouses, thermal stratification from the lower part of the vegetation zone to the upper part near the ceiling is usually formed and a high-temperature and stagnant flow region is observed, especially in the upper part, in greenhouses. The target zone of airflow and temperature control must be the vegetation zone, which is generally the lower part of greenhouses; therefore, the formation of thermal stratification indicates that the heating efficiency of a supplementary heating device is inefficient in winter.

This research focuses on an actual large-scale PVC greenhouse located in Japan, coupled CFD analysis of convection, radiation, and air-conditioning system is carried out in order to estimate the quantitative effects of the use of a stirred fan for air-mixing and an additional PVC screen for partitioning the upper and lower spaces on energy consumption.

Outline of target PVC greenhouse

The target greenhouse is a tunnel-type greenhouse, with two parallel tunnel-type sections, located in Japan. The inner dimensions of one side of the greenhouse are a width of roughly 6.3 m, a length of 86.0 m, and a maximum height of 3.4 m, as shown in Figure 1. There is no

partitioning wall between the two basic greenhouse units and a single non-partitioned space is present. The thickness of the PVC sheet acting as the outer wall is 0.1 mm. A photograph of the exterior, plan, and section are also shown in Figure 1.

In this parallel setting PVC greenhouse, an additional PVC screen can be installed for spatial partitioning of upper and lower zones. Additionally, stirred fans are also present in the upper part of the PVC greenhouse. The airflow rate of each stirred fan is 2,300 m^3/h and a heating source is not built into the fan; that is, it can just be operated to mix air.

A supplementary heating device, a hot-air furnace system, is placed in the greenhouse and temperature-controlled air is supplied through an air duct at six supply openings located at ground level during the night-time in winter. The total airflow rate of the hot-air furnace system is 27,600 m^3/h and the total heat output is 145 kW.

Outline of numerical analyses

The numerical analyses of airflow and temperature distribution in the PVC greenhouse during night-time in winter were carried out by Computational Fluid Dynamics (CFD). Additionally, CFD simulation that incorporated a feedback control routine of supply inlet temperature was carried out.

The flow fields were analyzed using the RNG k-ε model. The second-order upwind scheme was adopted for the convection term, and a SIMPLE algorithm was used for steady-state analyses. The temperature fields were analyzed on the basis of the coupled simulation of CFD, convective, conductive, and radiative heat transfers. Boussinesq approximation was adopted to reproduce the buoyancy effect. The view factors were analyzed by a hemicube method, and an iterative solution of radiosity method was used to analyze mutual radiation. For the PVC wall and the ground, one-dimensional heat-conductive analyses were carried out.

An outline of the analyzed space is given in Figure 1 and an unstructured tetramesh was used for a total of 558,794 meshes for CFD simulation.

CFD simulations in this study were performed with a commercial CFD software package, ANSYS FLUENT 12 (ANSYS, 2009). Table 1 indicates the boundary conditions for numerical analyses.

Feedback control method of supply inlet temperature

In order to estimate the optimal position of temperature sensors, a feedback routine between supply inlet air temperature and sensor temperature was incorporated into the CFD model.

The control method of the supply inlet air temperature is simple proportional control (P-control), as shown in equation 1.

$$T_{in}^{r} = T_{in} - K \times (T_{out} - T_{tar}) \quad (1)$$

Here, T_{tar} indicates target temperature (=15 °C in this analysis), T_{in} is supply inlet air temperature of each duct, T_{out} is the sensor temperature in space, and K denotes a proportional constant (=0.1 in this analysis).

The changes in supply inlet temperature and heat loads of the hot-air furnace in case the sensor position was changed were analyzed. The points of temperature sensors are depicted in Figure 1 (points A-C).

Numerical cases

Cases analyzed are shown in Table 2. The parameters of this analysis are with or without an additional PVC sheet for separating upper and lower parts of the greenhouse, a stirred fan for mixing air and eliminating thermal stratification, and a feedback control system between temperature sensors in the vegetation zone and supply inlet air temperature. A total of 8 analytical cases were arranged. The temperature sensor positions (points A, B, and C, and the average temperature of the vegetation zone) are indicated in Figure 1. The inlet velocity of

stirred fans is controlled at 5.5 m/s and turbulent intensity is 5% (recirculating airflow rate of each stirred fan is 2,300 m^3/h).

The temperature-conditioned air is supplied from duct openings, which are located at six points in the PVC greenhouse. The supply airflow rate of each inlet was set to 4,600 m^3/h and the average velocity was set to 5.0 m/s.

Results of numerical analysis

Results of flow and temperature fields

The prediction results of flow fields and temperature distribution for basic cases (Case 1-S – Case 2-S) are shown in Figures 2 and 3. In Case 1 without an additional PVC screen and a stirred fan, a stagnant flow field was formed in the entire space of the greenhouse, except for the vicinity of the supply inlet, and a non-uniform temperature distribution including a local high-temperature region was observed. In Case 2 with six operated stirred fans and an additional PVC screen, flow and temperaure fields were well mixed in the vegetation zone. The upper convection and diffusion of a supply jet from the stirred fan were restricted and the Coanda effect along the surface of the PVC screen was confirmed.

In all cases, the temperature-controlled air was supplied through supply inlets from six locations in the greenhouse; therefore, clear thermal stratification was not observed in the space. Gradual thermal stratification was confirmed in the vicinity of each supply inlet from the hot-air furnace.

Results of coupled analysis for CFD and feedback control of inlet air temperature

Table 3 and Figure 4 show summaries of the numerical results of average temperature and heat load of the hot-air furnace with incorporation of feedback control between supply inlet air temperature and sensor temperature. The flow and temperature distributions hardly changed from those of basic analytical cases (Cases 1-S-2-S).

In Case 1-A and Case 2-A in which the temperature sensor was located at position A as shown in Figure 1, relatively low-temperature air was supplied from the supply inlet (from a hot-air furnace). In Case 1-C and Case 2-C in which the temperature sensor was located at position C as shown in Figure 1, relatively high-temperature air was supplied from the supply inlet as a result of feedback control, regardless of the presence or absence of an additional PVC screen or a stirred fan. The maximum temperature difference of about 9 °C was caused by the difference in sensor positions in the greenhouse.

In Case 2 in which an additional PVC screen and stirred fan were incorporated, the average temperature in the vegetation zone became higher than the average temperature of the whole space. The introduction of an additional PVC screen into the greenhouse was effective for restricting the air-conditioning domain and increasing the heating efficiency.

The estimation results of supply heat load for each case are also shown in Table 3. The supply heat load was calculated by the following two methods: (i) all outdoor air is supplied to a hot-air furnace and there is no air returned to the hot-air furnace from the room, (ii) all returned air is supplied to the hot-air furnace and there is no outdoor air supplied to the hot-air furnace.

If the temperature sensor was set at point A, the supply heat load of the hot-air furnace decreased. In this case, the average temperature in the vegetation zone did not reach the target temperature of 15 °C. In contrast, with sensor point C, the supply heat load of the hot-air furnace increased relative to the previous example. In this case, the average temperature in the vegetation zone exceeded the target temperature by about 2 °C.

Differences of 30% to 40% in supply heat load were confirmed with the change of location of the temperature sensor.

The estimation results of fuel consumption of the hot-air furnace are shown in Table 4. The fuel consumption was estimated by the order of the supply heat load. Type A heavy oil

(Bunker A) was set as the fuel of the hot-air furnace. The ratio to the fuel consumption of a basic case is also shown in Table 4.

In the comparison between Case 1-A and Case 1-C, there was a 35% difference in fuel consumption. Since the averaged temperature in the vegetation zone in Case 1-A was about 3 °C lower than that in Case 1-C, the difference in energy consumption did not automatically indicate an energy-saving performance.

Conclusions

In this study, we reported the result of numerical analysis for flow and temperature distribution in a large-scale PVC greenhouse in winter. The findings obtained in this work can be summarized as follows:

(1) The space of environmental control became reduced in size upon the introduction of an additional PVC screen in the upper part of the vegetation region. The installation of the screen inside the large-scale vinyl house was a simple and energy-effective method of indoor environmental control.

(2) The air-mixing in a vertical direction and also in a horizontal direction in the large-scale PVC greenhouse was stimulated by the introduction of stirred fans in the upper region.

(3) From the viewpoint of heat load of the hot-air furnace system, the energy-saving effects of about 10 – 30% were confirmed upon introduction of a vinyl screen and a stirred fan in a large-scale PVC greenhouse. Because of the non-uniform distribution of temperature in the greenhouse, the position of temperature sensors strongly affected the energy consumption in the case where a feedback control system for the hot-air furnace was introduced.

Acknowledgement

This research was partly supported by a Grant-in-Aid for Scientific Research (JSPS KAKENHI for Young Scientists (S), 21676005). The authors would like to express special thanks to the funding source.

References

ANSYS, 2009. ANSYS FLUENT 12, ANSYS Japan Ltd.

Reichrath, S., Davies, T W., 2002. Using CFD to model the internal climate of greenhouses: past, resent and future, *Agronomie*, 22, pp3–10

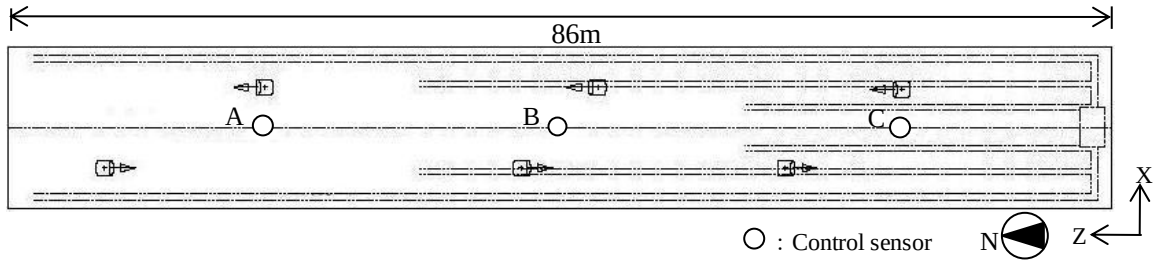

(1) Plan

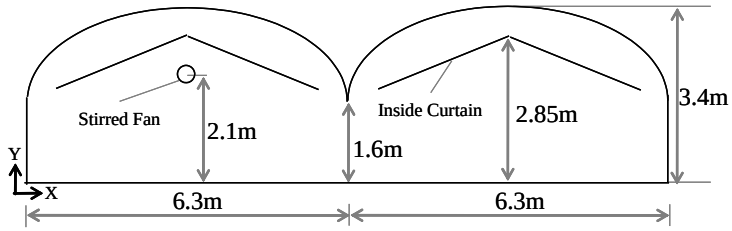

(2) Section

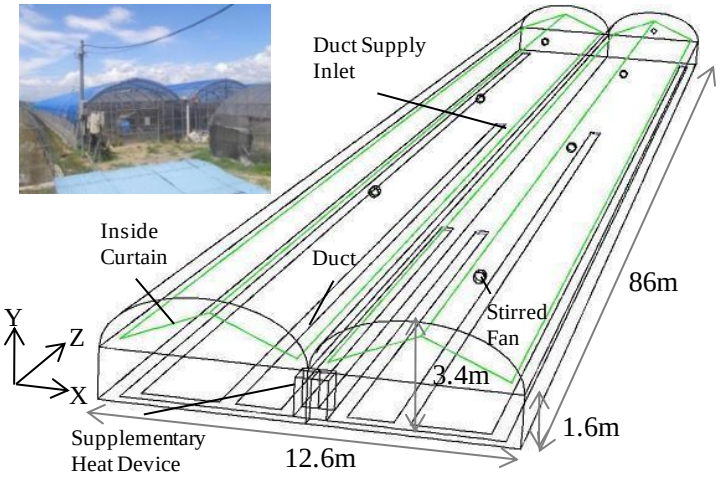

(3) Schematic geometry and photo of exterior

Figure 1 Outline of target greenhouse

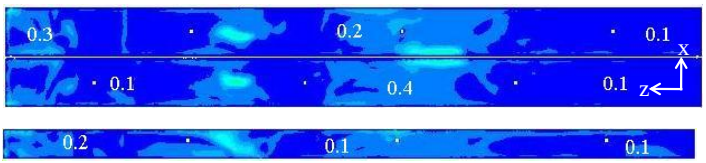

(1) Case 1-S (upper fig. : 2.1[m] from the ground, x-z plane / lower fig. : west center y-z section)

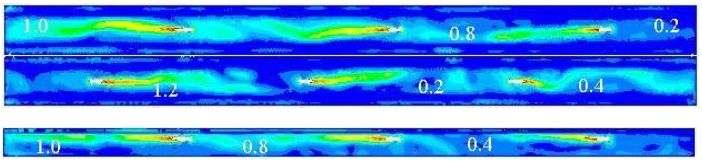

(2) Case 2-S (upper fig. : 2.1[m] from the ground, x-z plane / lower fig. : west center y-z section)

Figure 2 Air flow distribution (Results of CFD analyses)

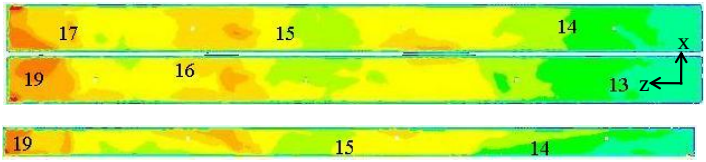

(1) Case 1-S (upper fig. : 2.1[m] from the ground, x-z plane / lower fig. : west center y-z section)

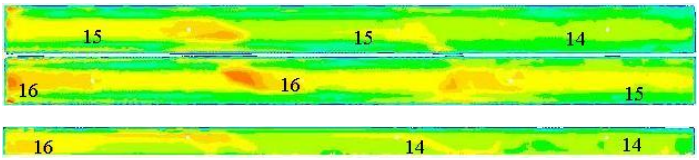

(2) Case 2 -S (upper fig. : 2.1[m] from the ground, x-z plane / lower fig. : west center y-z section)

Figure 3 Temperature distribution (Results of CFD analyses)

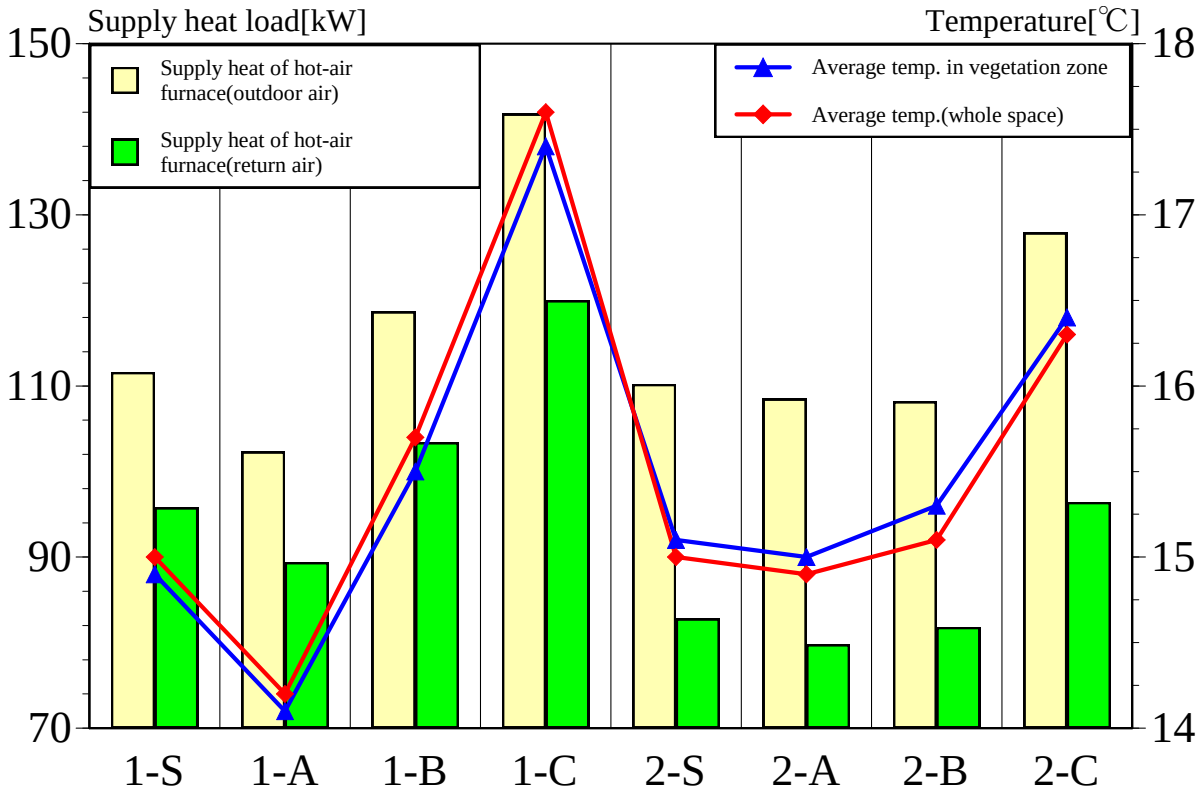

Figure 4 Results of total supply heat from hot-air furnace in case of coupled analysis with feedback simulation

Table 1 Boundary conditions for numerical analyses

Inflow	TI=5[%], L_{turb}=0.1 D_{JF}
Outflow	U_{out}=Free slip, k_{out}=Free slip, ε_{out}=Free slip
Outer Air	Sol-air temperature SAT : 4[°C] Outdoor air temperature : 9[°C] Convective heat transfer rate : 20[W/m^2/K]
Ground	Soil temperature at 1 m below ground : 10[°C], Thermal conductivity of soil : 1.0[W/m/k]
Inside Curtain	Thickness of PVC : 0.1[mm]
Duct	35[°C] constant as surface temperature
Duct Inlet	U_{in}=5.0[m/s], angle 30°
Wall Surface	Velocity : generalized log low Emissivity : 0.9

Table 2 Cases analyzed

Cases	PVC sheet for space partitioning	Stirred fan		Temperature sensor position	Supply air temperature of hot-air furnace
		Installed quantity	U_{inf} [m/s]		
Case 1-S	Not installed	0	-	Space average of vegetation zone	P-type control
Case 1-A				A (see Fig.1(1))	
Case 1-B				B (see Fig.1(1))	
Case 1-C				C (see Fig.1(1))	
Case 2-S	Installed (see fig. 1(3))	6	5.5	Space average of vegetation zone	
Case 2-A				A	
Case 2-B				B	
Case 2-C				C	

Table 3 The results of average air velocities and temperatures for Cases 1-S – 2-C (cases of feedback simulation)

Cases	PVC sheet for space partitioning	Stirred fan		Temp. sensor position	Average temp. in vegetation zone [°C]	Average temp. (whole space) [°C]	Supply inlet temp. from hot-air furnace	Supply heat of hot-air furnace (outdoor air temp. / return air temp.) [kW]	
		Installed quantity	U_{inf} [m/s]						
Case 1-S	Not installed	0	-	Space average of vegetation zone	14.9	15.0	25.7	111.6	95.8
Case 1-A				A (Fig.1(1))	14.1	14.2	23.6	102.3	89.4
Case 1-B				B (Fig.1(1))	15.5	15.7	27.3	118.7	103.4
Case 1-C				C (Fig.1(1))	17.4	17.6	32.5	141.8	120.0
Case 2-S	Installed	6	5.5	Space average of vegetation zone	15.1	15.0	25.7	110.2	82.8
Case 2-A				A	15.0	14.9	25.3	108.5	79.8
Case 2-B				B	15.3	15.1	25.4	108.2	81.8
Case 2-C				C	16.4	16.3	29.8	127.9	96.4

Table 4 The estimation results of fuel consumption of hot-air furnace

Cases	Consumption of heavy oil (type A) (outdoor air temp. / return air temp.) [L/h]		Ratio to Case 1-S (outdoor air temp. / return air temp.)	
Case 1-S	12.5	10.7	1.00	1.00
Case 1-A	11.4	10.0	0.92	0.93
Case 1-B	13.3	11.6	1.06	1.08
Case 1-C	15.8	13.4	1.27	1.25
Case 2-S	12.3	9.3	0.99	0.86
Case 2-A	12.1	8.9	0.97	0.83
Case 2-B	12.1	9.1	0.97	0.85
Case 2-C	14.3	10.8	1.15	1.01